

Fatigue Fractal Crack Propagating in a Self-Balanced Microstress Field

Andrea Carpinteri, Lorenzo Montanari, Andrea Spagnoli

Department of Civil-Environmental Engineering and Architecture, University of Parma
Viale Usberti 181/A, 43124 Parma, Italy; E-mail: spagnoli@unipr.it

ABSTRACT. *A kinked crack propagating in a periodic self-balanced multiaxial microstress field having self-similar characteristics is considered. The kinking angle of the crack is shown to depend on the properties of the microstress field. Using the Richardson's expression for self-similar fractals, the fractal dimension of the crack is expressed as a function of the kinking angle. Crack size effect on the fatigue crack growth rate in the Paris regime can be interpreted by the present model. Further, the Kitagawa diagram can be interpreted by showing that the threshold condition of fatigue crack growth is affected by the crack kinking angle which, in turn, is a function of the ratio between crack length and microstructure characteristic length.*

INTRODUCTION

During fatigue propagation, cracks tend to deflect as a result of far-field multiaxial stresses, microstructural inhomogeneities, residual stresses, dispersion of the material properties, and so forth (e.g. see Ref. [1]). Threshold condition and rate of fatigue crack growth appear to be significantly affected by the degree of deflection of cracks. This might be induced by the fact that the value of the near-tip stress intensity factors of kinked or branched fatigue cracks can be considerably different from that of a straight crack of the same projected length. With reference to two-dimensional elastic problems, analytical solutions for stress intensity factors of kinked cracks are available in the literature [2-5]. Some of such results have been used to gain a quantitative understanding of the relationship between the fatigue crack growth rate and the degree of deflection in the fatigue crack path (e.g. see Ref. [6]). In comparison to the highly idealised picture of a straight crack, a kinked crack represents a first step towards the description of actual irregularities of fracture surfaces. A further step in that direction is the use of the fractal geometry, as has been shown in several publications: for example, fractal geometry applications to size effect-related fatigue problems have been discussed in Refs [7-11].

In the present paper, following a recent work by the authors [12], the kinking angle is correlated to a periodic self-balanced multiaxial microstress field having self-similar characteristics. Using the Richardson's expression for self-similar fractals, the fractal dimension of the crack is expressed as a function of the kinking angle. Crack size effect on the fatigue crack growth rate in the Paris regime can be interpreted by the present model. Further, the Kitagawa diagram can be interpreted by showing that the threshold

condition of fatigue crack growth is affected by the crack kinking angle which, in turn, is a function of the ratio between crack length and microstructure characteristic length.

A KINKED CRACK IN A SELF-BALANCED MICROSTRESS FIELD

Stress Field and Projected SIFs

Let us consider an infinite plate (see Figs 1 and 2, where the y-axis is a symmetry axis for the crack), submitted to remote normal stress $\sigma^{(\infty)}$ along y-axis and shear stress $\tau^{(\infty)}$.

Assume the existence of a self-balanced microstress field, characterized by a material length d (for instance due to microstructural inhomogeneities, see Ref. [1]), with two non-zero stress components: a normal stress along the y-axis $\tilde{\sigma} = f(x/d)\tilde{\sigma}_a$ and a shear stress $\tilde{\tau} = f(x/d)\tilde{\tau}_a$. For the sake of simplicity, we assume $f(x/d) = \cos(2\pi x/d)$ (this could be regarded as a first order approximation through Fourier series of a general periodic function), Fig. 2. Under the uniform remote stresses $\sigma^{(\infty)}$ and $\tau^{(\infty)}$, the *remote* SIFs of the projected crack of semi-length l aligned with the x-axis are $K_I^{(\infty)} = \sigma^{(\infty)}\sqrt{\pi l}$ and $K_{II}^{(\infty)} = \tau^{(\infty)}\sqrt{\pi l}$. Under the self-balanced microstresses $\tilde{\sigma}$ and $\tilde{\tau}$, the *micro* SIFs of the projected crack are shown in Ref.[12] using the Buckner's superposition principle:

$$\begin{aligned}\tilde{K}_I &= 2\sqrt{\frac{l}{\pi}}\int_0^l \frac{\tilde{\sigma}}{\sqrt{l^2-x^2}}dx = 2\tilde{\sigma}_a\sqrt{\frac{l}{\pi}}\int_0^l \frac{\cos(2\pi x/d)}{\sqrt{l^2-x^2}}dx = \tilde{\sigma}_a\sqrt{\pi l}J_0\left(\frac{2\pi l}{d}\right) \\ \tilde{K}_{II} &= 2\sqrt{\frac{l}{\pi}}\int_0^l \frac{\tilde{\tau}}{\sqrt{l^2-x^2}}dx = 2\tilde{\tau}_a\sqrt{\frac{l}{\pi}}\int_0^l \frac{\cos(2\pi x/d)}{\sqrt{l^2-x^2}}dx = \tilde{\tau}_a\sqrt{\pi l}J_0\left(\frac{2\pi l}{d}\right)\end{aligned}\quad (1)$$

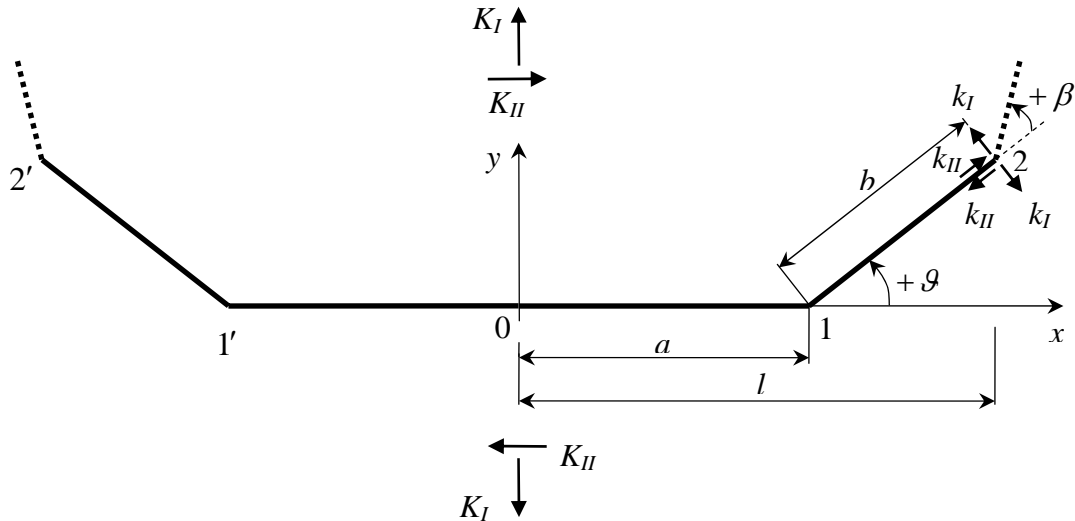


Figure 1. Kinked crack in an infinite plate.

where J_0 is the zero-order Bessel function. The total value of each *projected* SIFs is equal to the sum of the remote and micro stress contributions, that is, $K_I = K_I^{(\infty)} + \tilde{K}_I$, $K_{II} = K_{II}^{(\infty)} + \tilde{K}_{II}$.

Local SIFs and Kinking Criterion

During propagation in the above self-balanced multiaxial microstress field, the crack is assumed to kink at each reversal in the microstress spatial courses. Now, considering a periodically-kinked crack (of projected crack length $2l$), the *local* SIFs of the crack can be expressed through K_I and K_{II} as follows [5]:

$$\begin{aligned} k_I &= \cos^{3/2} \vartheta K_I - 2 \sin \vartheta \cos^{1/2} \vartheta K_{II} \\ k_{II} &= \sin \vartheta \cos^{1/2} \vartheta K_I + \cos 2\vartheta \cos^{-1/2} \vartheta K_{II} \end{aligned} \quad (2)$$

Note that Eq. 2 is based on the assumption that only the leading kinking angle of the periodically-kinked crack is influencing the local SIFs, and is valid (with good approximation) for $b/a > 0.3$ (a and b are shown in Fig.1). The classical criterion of Erdogan and Sih [13] is adopted to describe the mixed-mode crack propagation under the local SIFs k_I and k_{II} . Accordingly the kinking angle β , defined with respect to the generic inclined axis of the crack, is given by [13]:

$$\beta = 2 \arctan \left[\frac{1}{4} \frac{k_I}{k_{II}} \pm \frac{1}{4} \sqrt{\left(\frac{k_I}{k_{II}} \right)^2 + 8} \right] \quad (3)$$

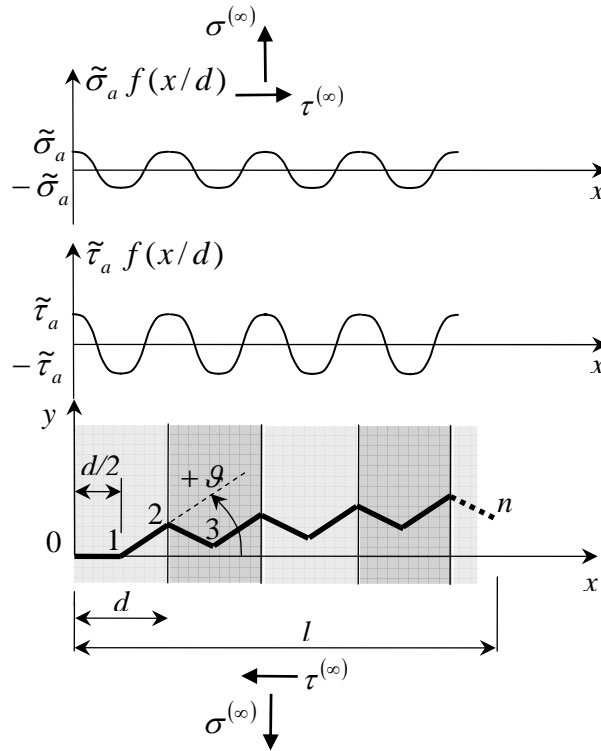


Figure 2. Self-balanced microstress field and periodically kinked crack.

EXTENSION TO MODE-I FRACTAL CRACKS UNDER FATIGUE LOADING

Now let us focus our attention on nominally Mode I cracks, i.e. cracks submitted to a remote Mode I cyclic loading. Hence, for an infinite plate, the SIF ranges related to the projected crack of semi-length l , according to Eq. 1, are given by:

$$\Delta K_I = \Delta \sigma^{(\infty)} \sqrt{\pi l} \left[1 + \frac{\Delta \tilde{\sigma}_a}{\Delta \sigma^{(\infty)}} J_0 \left(\frac{2\pi l}{d} \right) \right] \quad \Delta K_{II} = \Delta \sigma^{(\infty)} \sqrt{\pi l} \left[\frac{\Delta \tilde{\tau}_a}{\Delta \sigma^{(\infty)}} J_0 \left(\frac{2\pi l}{d} \right) \right] \quad (4)$$

where we assume that also the microstress field is time varying (e.g. $\Delta \tilde{\sigma}_a = \max_{t \in T} \tilde{\sigma}_a(t) - \min_{t \in T} \tilde{\sigma}_a(t)$) within the loading period T (constant amplitude fatigue loading).

Under the above loading conditions, cracks tend to propagate “on average” along the x axis following a zig-zag pattern, where the kinking angle ϑ is a function of the micro-to-remote stress ratios. In general, it turns out that the crack kinking angle decreases as the crack length increases with respect to the material microstructural length d , namely $\vartheta = \vartheta(l/d)$, Fig. 3a [12].

Self-Similarity

Considering a self-similar like microstress field, the zig-zag pattern of the crack shown in the previous Section is assumed to be followed in a self-similar manner at any scale of observation of the crack itself (Fig. 3b). The above assumption allows us to extend the above periodically-kinked crack model within the framework of the fractal geometry. Accordingly, following the fundamental Richardson’s expression [14], the fractal dimension D ($1 \leq D \leq 2$) is linked to the kinking angle ϑ :

$$D = \frac{\ln 2}{\ln(2 \cos \vartheta)} \quad (5)$$

The above relationship yields the limit values of $D = 1$ for $\vartheta = 0^\circ$ and $D = 2$ for $\vartheta = 45^\circ$, respectively. Since $\vartheta = \vartheta(l/d)$, Eq. 5 shows that the fractal dimension decreases as the crack length increases with respect to the material characteristic length (Fig. 3c).

Scale-Invariant SIF

From a reconsideration of the energetic approach by Griffith, it has been demonstrated that the SIF range for a fractal crack under Mode I fatigue loading is represented by the following scale-invariant quantity ΔK_I^* [8]:

$$\Delta K_I^* = \Delta K_I l^{\frac{1-D}{2}} \quad (6)$$

The physical dimensions of ΔK_I^* are dependent on the fractal dimension D , and are equal to $F \cdot L^{\frac{2+D}{2}}$, with F = force and L = length.

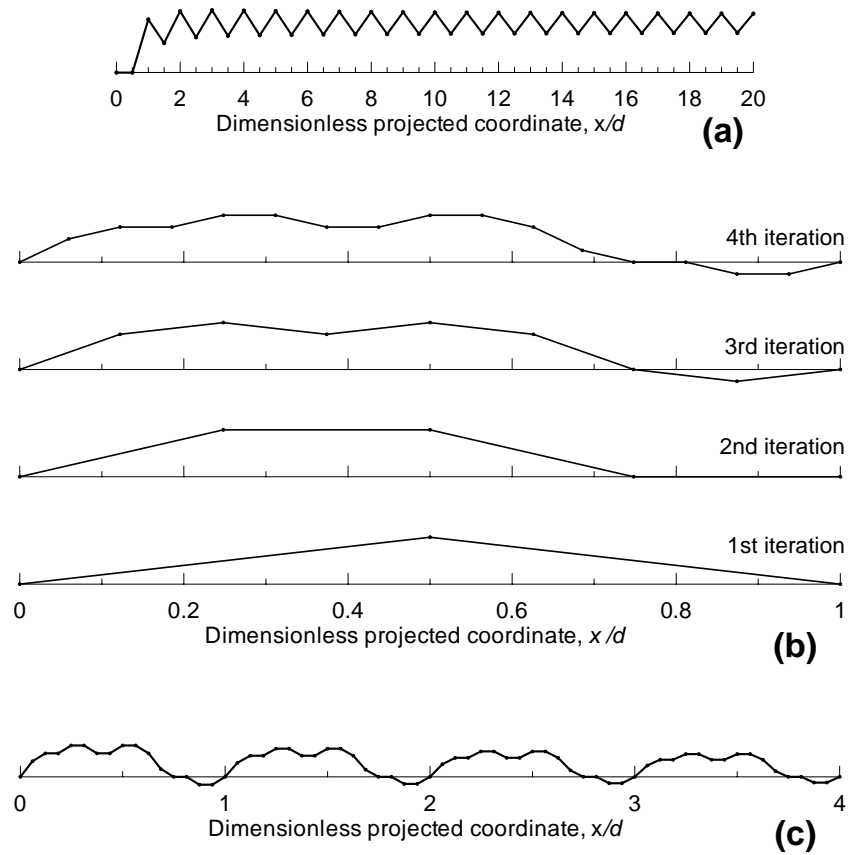


Figure 3. Illustrative sketches (not to scale) of: (a) A periodic zig-zag crack with kinking angle decreasing with increasing crack length; (b) First four iterations in the generation of a self-similar zig-zag crack; (c) A self-similar zig-zag crack at the 4th iteration with fractal dimension decreasing with increasing crack length.

Crack Growth Rate

Crack kinking induces a geometrical effect on crack growth rate. Since the fractal length of the crack l^* is equal to l^D , the derivation chain rule yields a relation between the scale-invariant crack growth rate dl^*/dN and its nominal counterpart dl/dN [8]:

$$\frac{dl^*}{dN} = \frac{dl^*}{dl} \frac{dl}{dN} = D l^{D-1} \frac{dl}{dN} \quad (7)$$

Fatigue Crack Growth Law

According to Ref. [8], the following modified Paris law can be used to describe the fatigue crack growth for a fractal crack

$$\frac{dl^*}{dN} = C (\Delta K_I^*)^m \quad (8)$$

where l^* is the renormalized crack length having physical dimension L^D .

By substituting Eqs 6 and 7 in Eq. 8, the following fatigue crack growth law in terms of the nominal quantities dl/dN and ΔK_I can be obtained [8] :

$$\frac{dl}{dN} = \left[\frac{C}{D} l^{(1-D)\left(1+\frac{m}{2}\right)} \right] \Delta K_I^m \quad (9)$$

Equation 9 explicitly depends on the crack length l and, hence, accounts for crack size effects on the fatigue crack growth rate. In other words, according to the classical Paris law, the fatigue crack growth rate implicitly depends on the crack length l because of the LEFM dependence of ΔK_I on l ($\Delta K_I \propto \Delta \sigma \sqrt{\pi l}$) and, in addition to such a $l^{0.5m}$ LEFM-dependence, a $l^{(1-D)(1+0.5m)+0.5m}$ fractal-dependence of the fatigue crack growth rate is proposed in the modified Paris law (Eq. 9). A thorough discussion of the variation of the fatigue crack growth rate as the crack length increases can be found in Ref. [8].

It is worth recalling that, during fatigue crack propagation, the increment of crack length might be small in comparison with the initial crack (or, in some case, notch) length. In such a case, the crack length l can be assumed constant during crack propagation and equal to the initial crack length and, therefore, the proposed modified Paris law in Eq. 9 describes, similar to the classical Paris law, a straight line with slope m in the bilogarithmic plot of dl/dN against ΔK_I .

TWO EXPERIMENTAL EVIDENCES OF CRACK SIZE EFFECTS IN FATIGUE

Fatigue Crack Growth

Assuming that the crack length l is smaller than a few times the microstress length scale d , the kinking angle ϑ of the zig-zag crack remains approximately constant according to the model described above. This yields self-similar fractal cracks, namely cracks having constant fractal dimension.

Based on this assumption, some experimental observations related to fatigue crack propagation in plain normal concrete and high-strength concrete [15, 16] can be described through Eq. 9. The maximum aggregate size, herein taken to be equal to the microstress length scale d , is equal to 12.7 and 9.5 mm for normal and high-strength concrete, respectively. The experimental tests, concerning 2D geometrically similar beams with an edge crack under pulsating three-point bending, show an evident crack size effect leading to different values of the Paris coefficient, function of the initial crack length, while the Paris exponent remains constant (details of the analysis of the experimental data [15, 16] can be found in Ref. [8]).

The experimental scale range is 1:4 and 1:8 for normal and high-strength concrete, respectively (that is, initial crack length ranging from 6.3 to 25.2 mm and from 6.3 to 50.4 mm for normal and high-strength concrete, respectively). The fitting of the experimental data leads to a power-type relationship between Paris coefficient (see term in square bracket of Eq. 9) and initial crack length. From such a relationship, the fractal

dimension of the crack can be extracted. For a nominally Mode I zig-zag crack propagating within a shear microstress field, the results are: (a) fractal dimension $D = 1.76$, kinking angle $\vartheta = 42^\circ$, micro-to-remote stress ratio $\Delta\tilde{\tau}_a/\Delta\sigma^{(\infty)} = 1.8$ for normal concrete; (b) $D = 1.27$, $\vartheta = 30^\circ$, $\Delta\tilde{\tau}_a/\Delta\sigma^{(\infty)} = 1.0$ for high-strength concrete.

Fatigue Threshold

Assuming that the crack length l can be much greater than the microstress length scale d , the kinking angle ϑ of the zig-zag crack decreases with increasing l , according to the model described above. This yields self-affine fractal cracks, namely cracks having a varying (decreasing in the present case) fractal dimension [14].

Based on this assumption, the experimental results obtained by Tanaka and co-workers [17] for mild steel plate specimens under fully reversed bending are herein interpreted through the proposed model. Such results are related to ferritic and pearlitic steels with carbon content of 0.20% and grain size (herein taken to be equal to the microstress length scale d) of the ferritic phase equal to 7.8 and 55 μm , respectively. For various values of the crack length (ranging from 6 to 1383 μm), the threshold stress intensity range ΔK_{Ith} is experimentally evaluated.

Figure 4 shows the comparison between experimental results (symbols) and theoretical curves (continuous line and dashed line). Such curves are obtained from the present model, see Eq. 6, considering $\Delta K_{Ith} = \Delta K_{Ith,0} l^{0.5(D-1)}$ ($\Delta K_{Ith,0}$ = fatigue threshold SIF range of long cracks, here assumed as the scale-invariant quantity; $\Delta K_{Ith,0}$ equal to 5.2 and 6.2 $\text{MPa}\sqrt{\text{m}}$ for small-size grain and large-size grain materials, respectively) and $\Delta\tilde{\tau}_a/\Delta\sigma^{(\infty)} = 2.07$ (this corresponds to $\vartheta = 45^\circ$ for $l/d \rightarrow 0$). Note that the value of ϑ , and hence of the fractal dimension D (see Eq. 5), decreases with l/d .

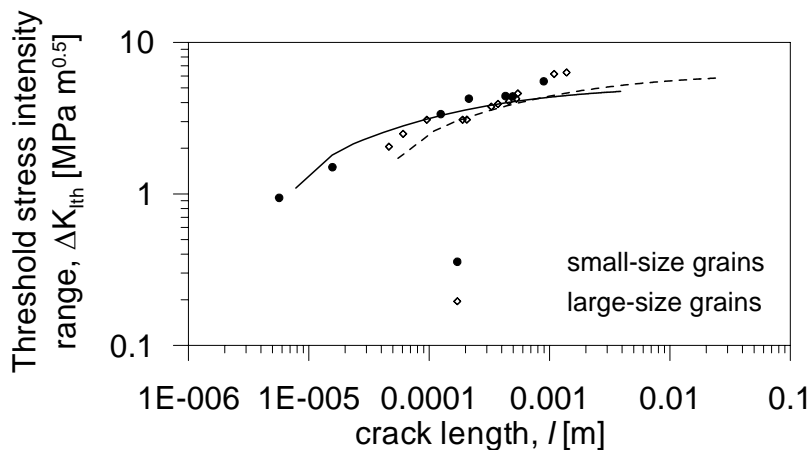


Figure 4. Experimental data [17] in the l - ΔK_{Ith} bilogarithmic plane and corresponding theoretical curves.

CONCLUSIONS

The presence of a periodic self-balanced microstress field is shown to produce a periodically-kinked crack path with a decreasing kinking angle as the crack length increases with respect to some material characteristic length. Such a periodically-kinked crack model is extended to fractal geometry using a self-similar generation procedure, so that the fractal dimension becomes a function of the kinking angle of the crack.

Crack size effect on the fatigue crack growth rate in the Paris regime (that is, at equal SIF range, the rate decreases as the crack length increases) can be interpreted by the present model. Further, the model offers a theoretical basis (within the framework of the fractal geometry) to explain the variation of fatigue threshold condition with the crack length (Kitagawa diagram).

REFERENCES

1. Brighenti, R., Carpinteri, A., Spagnoli, A., Scorza, D. (2012) *Frattura ed Integrità Strutturale* **20**, 6-16.
2. Kitagawa, H., Yuuki, R., Ohira T. (1975) *Engng Fract Mechs* **7**, 515-529.
3. Lo, K.K. (1978) *J Applied Mechs* **45**, 797-802.
4. Suresh, S., Shih, C.F. (1986) *Int J Fract* **30**, 237-259.
5. Chen, Y.Z. (1999) *Theoretical Applied Fract Mechs* **31**, 223-232.
6. Suresh, S. (1985) *Metallurgical Trans* **14A**, 2375-2385.
7. Carpinteri, A., Spagnoli, A., Vantadori, S. (2002) *Fatigue Fract Engng Mater Structs* **25**, 619-627.
8. Carpinteri, A., Spagnoli, A. (2004) *Int J Fatigue* **26**, 125-133.
9. Spagnoli, A. (2004) *Chaos, Solitons and Fractals* **22**, 589-598.
10. Spagnoli, A. (2005) *Mechs Mater* **37**, 519-529.
11. Carpinteri, A., Spagnoli, A., Vantadori, S., Viappiani, D. (2008) *Engng Fract Mechs* **75**, 579-589.
12. Carpinteri, A., Spagnoli, A., Vantadori, S. (2011) In: *The 13th International Congress on Mesomechanics (Mesomechanics 2011)*, Vicenza (Italy).
13. Erdogan, F., Sih, G.C. (1963) *J Basic Engng* **85**, 519-527.
14. Mandelbrot, B.B. (1982) *The fractal geometry of nature*. New York: W.H. Freeman and Company.
15. Bazant, Z.P., XU, K. (1991) *ACI Materials J* **88**, 390-399.
16. Bazant, Z.P., Shell, W.F. (1993) *ACI Materials J* **90**, 472-478.
17. Tanaka, K., Nakai, Y., Yamashita, M. (1981) *Int J Fatigue* **17**, 519-33.